



Distributed Data-Driven Control of Transportation Networks

Vladimir Toro, Eduardo Mojica-Nava, Naly Rakoto-Ravalontsalama

► To cite this version:

Vladimir Toro, Eduardo Mojica-Nava, Naly Rakoto-Ravalontsalama. Distributed Data-Driven Control of Transportation Networks. MIM 2022: IFAC Conference on Manufacturing Modelling, Management and Control, Jun 2022, Nantes, France. pp.239-244, 10.1016/j.ifacol.2022.09.395 . hal-03860561

HAL Id: hal-03860561

<https://hal.science/hal-03860561>

Submitted on 24 Nov 2022

HAL is a multi-disciplinary open access archive for the deposit and dissemination of scientific research documents, whether they are published or not. The documents may come from teaching and research institutions in France or abroad, or from public or private research centers.

L'archive ouverte pluridisciplinaire **HAL**, est destinée au dépôt et à la diffusion de documents scientifiques de niveau recherche, publiés ou non, émanant des établissements d'enseignement et de recherche français ou étrangers, des laboratoires publics ou privés.



Distributed under a Creative Commons Attribution - NonCommercial - NoDerivatives 4.0 International License

Distributed Data-Driven Control of Transportation Networks

Vladimir Toro* Eduardo Mojica-Nava*
Naly Rakoto-Ravalontsalama**

* Universidad Nacional de Colombia, Bogota, 111321, e-mail:
bwtorot@unal.edu.co, eamojican@unal.edu.co.

** IMT Atlantique, Nantes, France, 44307, e-mail:
naly.rakoto@imt-atlantique.fr

Abstract: This paper presents a data-driven control for a network of autonomous vehicles. The general scheme of cruise control is implemented for a set of vehicles defined by a nonlinear equation. Koopman operator allows representing the nonlinear system in the Koopman space (lifted space), suitable to get a linear observer that is used for distributed control instead of the nonlinear model. The proposed control simplified the control design and also allows to use a linear Model Predictive Control (MPC) in a distributed form.

Copyright © 2022 The Authors. This is an open access article under the CC BY-NC-ND license (<https://creativecommons.org/licenses/by-nc-nd/4.0/>)

Keywords: Koopman operator, cruise control, data-driven, distributed control

1. INTRODUCTION

The problem of traffic control in transport networks is relevant due to the increase in merchandising and the necessity of reducing human error and misbehavior on urban routes. In both cases, improvements in vehicle technologies make possible the study of control algorithms that allow regulating the flow of vehicles. Autonomous cruise control (ACC) and Cooperative ACC (CCAC) are well studied techniques to regulate the flow of vehicles; they are supported by a set of equations that define the relation of the magnitudes of the vehicle and its interaction with the environment and other vehicles Van Arem et al. (2006). These differential equations are nonlinear, which are linearized for control design in several cases. However, this limits the range in which control parameters hold, and may omit critical behaviors of vehicle dynamics.

A general model of the vehicle dynamics given by the torque applied and the effect of gravity, mass, and route interactions with the tires can be used to define a cruise control independent of the source of power of the vehicle (electric, hybrid, gas) Shakouri et al. (2010). The controller should allow to control the velocity of the vehicle and, at the same time, to optimize the torque produced by the engine, while keeping the restriction of distance. Several studies have been done for CCAC applying different control techniques and approaches. Milanés et al. (2014) designs a CCAC using a linear model of the vehicle. Naus et al. (2010) presents a condition for a CCAC for string stability and considering heterogeneity (different characteristics). A nonlinear model predictive control (NMPC) is designed by Shakouri and Ordys (2014), in which the controllers have the capability of switching between CACC and ACC depending on the situation. A model-free approach is presented by Zhao et al. (2017), and Lin et al. (2021) in which Reinforcement Learning (RL) techniques

are used to learn an optimal policy following an actor-critic structure. In any case, the optimization process over a nonlinear model may be difficult due to the non-convexity of the space, resulting in extra computation time and additional restrictions. In contrast, the data available coming from sensors and detailed simulation models increases the interest in data-driven techniques.

Some RL techniques use a black-box structure, which can be problematic for determining stability Kiumarsi et al. (2018). Another data-driven approach is the one based on operators. Among them, the Koopman operator has called the attention in recent years, together with its dual operator known as the Perron-Frobenius operator Mezic (2005). The main advantage of the Koopman operator is its capability of representing nonlinear dynamical systems as a linear one in a new space known as the space of observables, lifted-space, or Koopman space. Such capability of linear representation has been enhanced by the development of data-based algorithms that only use measurements of the system and have been optimized to reduce the computation time and the necessity of data arrangement before using them.

ACC only needs limited information; however, in CCAC each vehicle gathers information from other vehicles according to the communication network. This distributed approach allows taking decisions based only on local information. However, the coupling between physical magnitudes should be problematic for control design. The linear representation in the lifted space facilitates the optimal control design, following the distributed approach while keeping the restrictions of the system.

This paper is organized as follows: Section 2 presents the nonlinear model for cruise control of vehicles. Section 3 presents the generalities of the Koopman operator and

the data-driven EDMD algorithm. The distributed control design using the Koopman model is presented in Section 4. Section 5 presents a case study with the simulation results. Finally, conclusions are presented in Section 6.

2. NONLINEAR MODEL FOR CRUISE CONTROL

Autonomous cruise control for vehicles is based on differential equations representing the interactions of the vehicle with the environment, and the model of the torque source or motor Shakouri et al. (2012), Shakouri and Ordys (2014). In Shakouri et al. (2010), it is presented a very detailed model which includes the engine, the torque converter, and the gearbox for the vehicle, and the external forces acting over it, such as the gravitational effects, the rolling resistance, and the aerodynamic drag.

Here, it is used a general model which includes the torque as controlled input and the velocity of the car as state-variable, like the used by Orosz and Shah (2012) as follows

$$m_{\text{eff}}\dot{v} = -mg \sin \phi - \gamma mg \cos \phi - k(v + v_w)^2 + \frac{\eta}{R} T_{\text{en}} \quad (1)$$

where $m_{\text{eff}} = m + \frac{J}{R^2}$ is the effective mass that gathers the mass of the vehicle m , the moment of inertia J , and the wheel radius R . The gravitational constant is given by g , ϕ is the inclination angle, γ is the rolling resistance coefficient, k is the air drag constant, the velocity of the headwind is given by v_w , η is the gear ratio, and the engine torque is given by T_{en} .

Assuming $\phi = 0$, $v_w = 0$, and $J = 0$, (1) is simplified as

$$m\dot{v} = -\gamma mg - kv^2 + \frac{\eta}{R} T_{\text{en}} \quad (2)$$

which is very suitable for determining the set of observables, as will be explained in the next sections.

Interacting vehicles Model (1) represents the dynamic of a single vehicle. However, some assumptions should be made for the proper control of a set of vehicles.

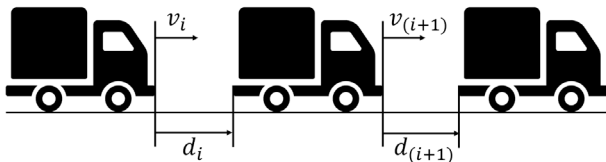


Fig. 1. Single lane sequence of vehicles and definitions for cruise control

Assumption 1 Based on Fig.1, a single lane of vehicles is considered, and aside from the inherent differences among them, such as the weight and the tire features, it is considered that the dynamics of all vehicles are identical.

Assumption 2 Distances among vehicles d_i are given by the difference between tail and head among them, and there is a leader vehicle denoted by L with velocity denoted by V_L .

Assumption 3 It is assumed a wireless communication system without delay for the distributed control.

The distance among vehicles is given by the difference between tail and head of each vehicle. The distance between the leader and the first vehicle behind is given by

$$\dot{d}_i = V_L - v_i \quad (3)$$

It is also possible to define the desired distance between vehicles as

$$d_{\text{des}} = l + d_s + T_h V_i \quad (4)$$

where l is the vehicle length, d_s is the desired distance between vehicles, also known as the collision distance, and T_h is the constant-time headway which is defined between 1.5s and 2s by Martinez and Canudas-de Wit (2007).

3. KOOPMAN OPERATOR AND EDMD

The Koopman operator or composition operator is related to methods to deal with nonlinear systems representing them as linear ones but of infinite dimension. Koopman operator is the dual of the Perron-Frobenius operator that has been used in statistical mechanics. The increasing interest in the Koopman operator comes from its capacity for showing properties of nonlinear systems, such as ergodicity and periodicity. Koopman operator can be defined for discrete-time and continuous-time systems Mauroy et al. (2020).

For a discrete-time dynamical system defined by

$$x_{k+1} = Sx_k$$

where S defines the nonlinear transformation $S : X \rightarrow X$, and X is a finite-dimensional metric space. The evolution of the system is described by the nonlinear transformation $\mathbf{S}^k(x)_{k=0}^\infty$ with initial condition x_0 . Also, it is defined a set of functions known as observables or basis functions $f : X \rightarrow \mathbb{C}$. The Koopman operator is defined as

$$U_s f = f \circ S \quad \forall f \in \mathcal{F}$$

where \mathcal{F} is the space of observables usually defined by a Banach space.

Koopman eigenvalues and eigenfunctions Koopman operator allows defining a set of eigenfunctions and eigenvalues for discrete and continuous systems. An eigenfunction is an observable ϕ_μ of the Koopman operator with a discrete-map S that satisfies

$$U\phi_\mu = \phi_\mu \circ S = \mu\phi_\mu$$

where $\mu \in \mathbb{C}$ is the associated eigenvalue Mauroy et al. (2020).

Koopman modes The Koopman mode expansion of $f \in \mathcal{G}$ where $\mathcal{G} \subseteq \mathcal{F}$, and assuming that the span of Koopman eigenfunctions $\phi_{\mu j}_{j=1}^\infty$ is given by

$$f = \sum_{j=1}^{\infty} v_j \phi_{\mu j}$$

where v_j are the Koopman modes corresponding to the observable f . Koopman expansion can be applied to this expression as follows

$$U^k f = \sum_{j=1}^{\infty} v_j \mu_j^k \phi_{\mu j} \quad (5)$$

3.1 Data-Driven methods and EDMD

Koopman mode decomposition (KMD) given by (5) can be determined by different methods, among them generalized Laplace averages Mauroy et al. (2020), and finite dimensional matrix approximation with techniques such as Dynamic Mode Decomposition (DMD) and Extended DMD (EDMD).

Suppose a set of M measurements of the form $\{x_k, y_k\}_{k=1}^M$ where $y_k = S(x_k)$, and a set of N observables or basis functions $\{\psi_1, \psi_2, \dots, \psi_N\}$, the next two matrices are defined

$$X = [\psi_1(x), \psi_2(x), \dots, \psi_N(x)]$$

$$Y = [\psi_1(y), \psi_2(y), \dots, \psi_N(y)]$$

Then the Koopman matrix U is given by

$$U = X^\dagger Y$$

where X^\dagger is the pseudo-inverse of X .

For a system with inputs, the Koopman operator can be determined by

$$(Uf)(x, u) = f(S(x, u), u).$$

where u is the control input.

4. DISTRIBUTED DATA-DRIVEN PREDICTIVE CONTROL

It is possible to build a linear predictor based on the Koopman representation of a nonlinear system given by matrices \mathcal{A} , \mathcal{B} , and \mathcal{C} as the one presented by Korda and Mezić (2018)

$$\begin{aligned} z_{k+1} &= \mathcal{A}z_k + \mathcal{B}u \\ y &= \mathcal{C}z \end{aligned} \quad (6)$$

with $z_0 = \psi(x_0)$.

Equation for the distance between vehicles given by (3) is discretized using the Euler method as follows

$$d_{k+1}^i = d_k^i + T(V_L - z_k^i).$$

where T is the sampling time.

Linear predictor (6) approximates the nonlinear behavior of (1). The approximation holds for a set of samples; the better the approximation, the greater the number of

samples that it holds. The leader vehicle sets the velocity for the rest of vehicles, then the optimization problem is written as

$$\begin{aligned} \min_{u^l} \quad & \sum_{k=0}^{H_p} \|z_{t+k}^l - z_{t+k}^{ref}\|_Q^2 + \|u_{t+k}^l\|_R^2 \\ \text{s.t.} \quad & z_{k+1}^l = z_k^l + T(\mathcal{A}z_k^l + \mathcal{B}u^l) \end{aligned} \quad (7)$$

where H_p is the prediction time-horizon, Q is the gain related to the state difference with the reference value, R is the gain related to the input, and l denotes the leader node with velocity reference value $z^{ref,l}$.

The distance between vehicles is given by the sum of the distance calculated by using (4), and the desired distance between vehicles is defined as follows

$$d_{inter} = d^i + d_s.$$

For the rest of vehicles, the optimization problem should include the restriction for the distance between vehicles, based on the control proposed by Orosz and Shah (2012) the velocity of each vehicle depends on the distance between the vehicle and the vehicle in front of it. Then, the next control law is proposed

$$f(x) = \begin{cases} 0, & \text{if } d_{inter} \leq d_s \\ u^i, & \text{if } d_{inter} > d_s \end{cases}$$

where u^i is given by solving the next optimization problem

$$\begin{aligned} \min_{u^i} \quad & \sum_{k=0}^{H_p} \|z_{t+k}^i - z_{t+k}^{ref}\|_Q^2 + \|u_{t+k}^i\|_R^2 + \|\mathcal{L}(:, i)\mathbf{z}\|_S^2 \\ \text{s.t.} \quad & z_{k+1}^i = z_k^i + T(\mathcal{A}z_k^i + \mathcal{B}u^i) \end{aligned} \quad (8)$$

where $\mathbf{z} = [z_1 \ z_2 \ \dots \ z_n]^\top$ is a vector with the values of each vehicle, $\mathcal{L}(:, i)$ is the i^{th} row of the Laplacian matrix \mathcal{L} , and S is the gain value for the consensus term.

5. CASE STUDY

Dynamic model (1) is simulated in Matlab according to the particular characteristics of each vehicle. Series of data are generated by simulation and used to determine the Koopman operator. Data is sampled each $T_s = 0.1$ s with a simulation horizon of $T_h = 10000$ s generating 100000 samples. The initial conditions vary randomly from $[0, 100]$ each 200s; the control input varies from $[500, 1500]$ each 87s. A set of 990 samples with a unique initial condition is used for verification purposes.

The simulation scenario consists of seven vehicles with different mass, tire rolling coefficients, and tire radius. These values are shown in Table 1. The general parameters of the system are shown in Table 2.

The set of observables or basis functions is given by

$$\Phi = [1 \quad v \quad v^2 \quad \exp(0.1v) \quad \sin(v) \quad \cos(v)]$$

Table 1. Vehicles Parameters

Vehicle index	Mass (kg)	TRRC (γ)	TRR(R) (m)
1	1555	3.5	0.313
2	1849.1	2.8	0.322
3	1934.0	3.6	0.283
4	1678.7	2.9	0.337
5	1757.7	2.5	0.293
6	1743.1	3.3	0.276
7	1392.2	3.1	0.301

TRRC: Tire rolling resistance coefficient

TRR: Tire rolling radius

Table 2. System Parameters

Vehicle feature	Value
Gravitational acceleration m/s^2	$g = 9.81$
Desired maximum velocity m/s	$v_{max} = 30$
Desired distance m	$d_s = 23$
Minimal free flow distance m	$h_{go} = 35$
kg/m	$k = 0.463$

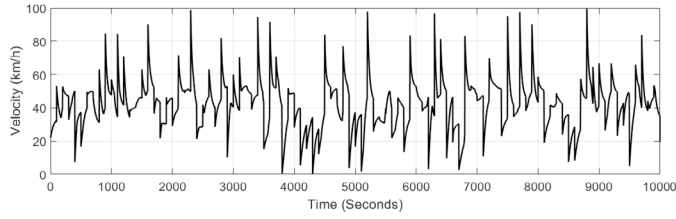


Fig. 2. Velocity output generated by varying the initial conditions and control input

$$A_1 = \begin{bmatrix} 1.0000 & -0.0000 & 0.0000 & -0.0000 & 0.0000 & 0.0000 \\ -0.0154 & 1.0006 & -0.0000 & 0.0000 & 0.0051 & -0.0009 \\ -8.8259 & 0.4721 & 0.9910 & -0.0000 & 0.3438 & -0.5066 \\ -0.0444 & -0.1382 & 0.0040 & 0.9789 & -0.0763 & -1.4405 \\ -0.0038 & 0.0002 & -0.0000 & 0.0000 & 0.9985 & -0.0039 \\ 0.0010 & -0.0000 & 0.0000 & 0.0000 & 0.0042 & 0.9983 \end{bmatrix};$$

$$B_1 = \begin{bmatrix} 0.0000 \\ 0.0001 \\ 0.0065 \\ 0.0026 \\ 0.0000 \\ 0.0000 \end{bmatrix}; \quad C_1 = [0 \ 1 \ 0 \ 0 \ 0 \ 0].$$

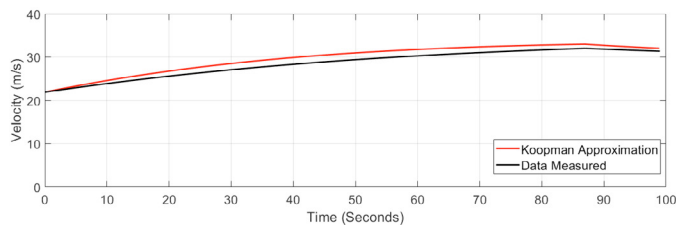


Fig. 3. Koopman approximation and data measured representation

Matrices A , B , and C are found using the EDMD algorithm. The system response of the linear observer and using the set of data for verification is shown in Fig. 3. The first values fit better with the data measured, while as time passes, the approximation deviates from the real values.

The parameters for the MPC are shown in Table 3., these values are applied to all vehicles, including the leader.

Table 3. MPC Parameters

MPC Feature	Value
Prediction Horizon	$H_p = 30$
State-variable gain	$Q = 1 \times 10^7$
Input gain	$R = 1$
Consensus gain	$S = 1$
Sampling time	$T_s = 0.5\text{s}$
Control signal constraint	$-8 \times 10^3 \leq u \leq 8 \times 10^3$

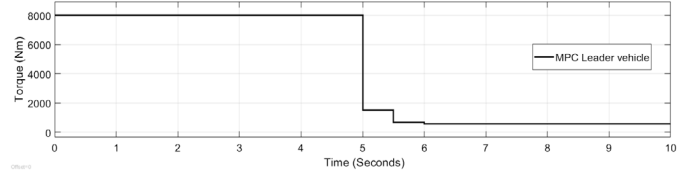


Fig. 4. Control signal (Torque applied) to the leader vehicle

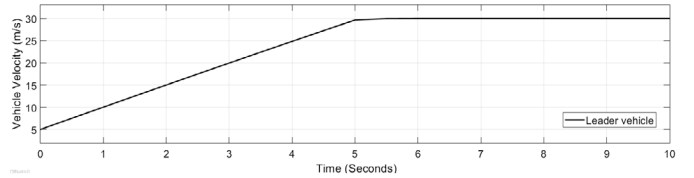


Fig. 5. Change of speed for the leader vehicle when applying the predictive controller, the set point is 30m/s

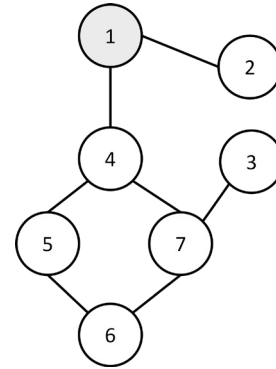


Fig. 6. Graph for communication among vehicles

The control signal applied to the leader vehicle is shown in Fig. 4. The control signals (torque) are limited to two values in which negative torque corresponds to the action of the brakes. The velocity of the leader vehicle is shown in Fig. 5. It takes a few seconds to reach the desired velocity.

Communication among vehicles is represented by the graph shown in Fig. 6. The leader node appears in shadow. Connections among agents are determined by the adjacency (Adj) and Laplacian matrix \mathcal{L} of the graph as follows

$$Adj = \begin{bmatrix} 0 & 1 & 0 & 1 & 0 & 0 & 0 \\ 1 & 0 & 0 & 0 & 0 & 0 & 0 \\ 0 & 0 & 0 & 0 & 0 & 0 & 1 \\ 1 & 0 & 0 & 0 & 1 & 0 & 1 \\ 0 & 0 & 0 & 1 & 0 & 1 & 0 \\ 0 & 0 & 0 & 0 & 1 & 0 & 1 \\ 0 & 0 & 1 & 1 & 0 & 1 & 0 \end{bmatrix}$$

$$\mathcal{L} = \begin{bmatrix} 2 & -1 & 0 & -1 & 0 & 0 & 0 \\ -1 & 1 & 0 & 0 & 0 & 0 & 0 \\ 0 & 0 & 1 & 0 & 0 & 0 & -1 \\ -1 & 0 & 0 & 3 & -1 & 0 & -1 \\ 0 & 0 & 0 & -1 & 2 & -1 & 0 \\ 0 & 0 & 0 & 0 & -1 & 2 & -1 \\ 0 & 0 & -1 & -1 & 0 & -1 & 3 \end{bmatrix}$$

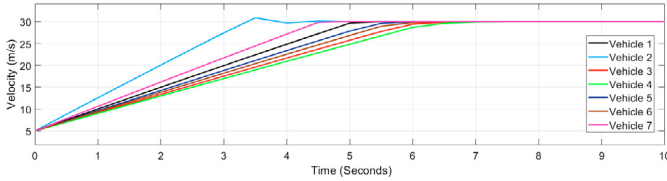


Fig. 7. Velocity response for each of the seven vehicles simulated. All vehicles reach the reference of 30m/s

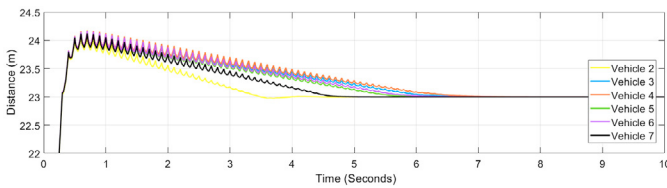


Fig. 8. Distance of the vehicles behind the leader, the desired distance is set to 23m which is reach in a few seconds.

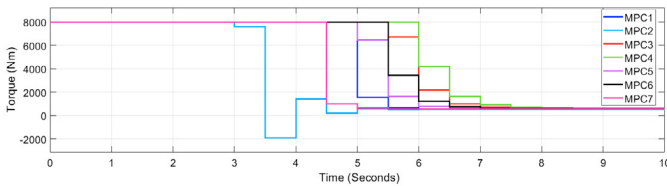


Fig. 9. Model predictive control signals applied to the seven vehicles.

The leader vehicle determines the velocity of the rest of vehicles, after applying the control law (8), reach the reference value in a few seconds. The desired distance between vehicles is set to be 23m as it is shown in Fig. 8. Each vehicle reaches this value by applying the control rule. The seven predictive control signals are shown in Fig.9. The controller holds for a few seconds a high torque, and then this value drops until the vehicle achieves the references for velocity and distance.

6. CONCLUSION

This paper presents a cruise control for a network of autonomous vehicles following a distributed data-driven control approach. The general scheme of cruise control is implemented for a set of vehicles defined by a nonlinear equation. Nonlinearities are managed by representing the equation in the Koopman space; this allows to get a linear observer that is used for distributed control instead of the nonlinear model. The proposed control simplified the control design and also allows to use a linear MPC. As a future work, the distributed problem can be solved by an alternating algorithm such as the distributed alternating direction multiplier method (ADMM), or use learning methods to determine the observable functions for the Koopman representation.

REFERENCES

- Kiumarsi, B., Vamvoudakis, K.G., Modares, H., and Lewis, F.L. (2018). Optimal and Autonomous Control Using Reinforcement Learning: A Survey. *IEEE Transactions on Neural Networks and Learning Systems*, 29(6), 2042–2062. doi:10.1109/TNNLS.2017.2773458.
- Korda, M. and Mezić, I. (2018). Linear predictors for nonlinear dynamical systems: Koopman operator meets model predictive control. *Automatica*, 93, 149–160. doi: 10.1016/j.automatica.2018.03.046.
- Lin, Y., McPhee, J., and Azad, N.L. (2021). Comparison of Deep Reinforcement Learning and Model Predictive Control for Adaptive Cruise Control. *IEEE Transactions on Intelligent Vehicles*, 6(2), 221–231. doi: 10.1109/TIV.2020.3012947.
- Martinez, J.J. and Canudas-de Wit, C. (2007). A safe longitudinal control for adaptive cruise control and stop-and-go scenarios. *IEEE Transactions on Control Systems Technology*, 15(2), 246–258. doi: 10.1109/TCST.2006.886432.
- Mauroy, A., Susuki, Y., and Mezić, I. (2020). *Introduction to the koopman operator in dynamical systems and control theory*, volume 484. Springer International Publishing.
- Mezic, I. (2005). Spectral properties of dynamical systems, model reduction and decompositions. *Nonlinear Dynamics*, 41, 309–325. doi:10.1007/s11071-005-2824-x.
- Milanes, V., Shladover, S.E., Spring, J., Nowakowski, C., Kawazoe, H., and Nakamura, M. (2014). Cooperative adaptive cruise control in real traffic situations. *IEEE Transactions on Intelligent Transportation Systems*, 15(1), 296–305. doi:10.1109/TITS.2013.2278494.
- Naus, G.J., Vugts, R.P., Ploeg, J., Van De Molengraft, M.J., and Steinbuch, M. (2010). String-stable CACC design and experimental validation: A frequency-domain approach. *IEEE Transactions on Vehicular Technology*, 59(9), 4268–4279. doi:10.1109/TVT.2010.2076320.
- Orosz, G. and Shah, S.P. (2012). A nonlinear modeling framework for autonomous cruise control. *ASME 2012 5th Annual Dynamic Systems and Control Conference Joint with the JSME 2012 11th Motion and Vibration Conference, DSCC 2012-MOVIC 2012*, 2(ii), 467–471. doi:10.1115/DSCC2012-MOVIC2012-8871.
- Shakouri, P., Ordys, A., Askari, M., and Laila, D.S. (2010). Longitudinal vehicle dynamics using Simulink/Matlab. *IET Seminar Digest*, 2010(4), 955–960. doi:10.1049/ic.2010.0410.
- Shakouri, P. and Ordys, A. (2014). Nonlinear Model Predictive Control approach in design of Adaptive Cruise Control with automated switching to cruise control. *Control Engineering Practice*, 26(1), 160–177. doi: 10.1016/j.conengprac.2014.01.016.
- Shakouri, P., Ordys, A., and Askari, M.R. (2012). Adaptive cruise control with stop&go function using the state-dependent nonlinear model predictive control approach. *ISA transactions*, 51(5), 622–631. doi: 10.1016/j.isatra.2012.05.001.
- Van Arem, B., Van Driel, C.J., and Visser, R. (2006). The impact of cooperative adaptive cruise control on traffic-flow characteristics. *IEEE Transactions on Intelligent Transportation Systems*, 7(4), 429–436. doi: 10.1109/TITS.2006.884615.

Zhao, D., Xia, Z., and Zhang, Q. (2017). Model-Free Optimal Control Based Intelligent Cruise Control with Hardware-in-the-Loop Demonstration [Research Frontier]. *IEEE Computational Intelligence Magazine*, 12(2), 56–69. doi:10.1109/MCI.2017.2670463.